

Crutchley, G.J., et al., 2018, How tectonic folding influences gas hydrate formation: New Zealand's Hikurangi subduction margin: *Geology*, <https://doi.org/10.1130/G45151.1>

Supplement A: Seismic acquisition and processing:

The PEG09 and APB13 seismic data used in this study were processed by CGG Services (Singapore) Pte. Ltd under contract to Anadarko New Zealand Company in 2014. Anadarko New Zealand Company was the operator of exploration permits PEP54858 and PEP54861 in the Pegasus Basin, on New Zealand's offshore East Coast. The following information about acquisition parameters and processing has been extracted from Petroleum Reports^[1-3] available from New Zealand Petroleum and Minerals, which is part of New Zealand's Ministry for Business, Innovation and Employment. At the time of publishing this paper, the reports, and data, can be accessed from: <https://www.nzpam.govt.nz/maps-geoscience/exploration-database/>

Acquisition parameters:

PEG09 Survey	
Vessel	<i>M/V Reflect Resolution</i>
No. of channels	800
Group length	12.5 m
Offset - source to Channel 1	140 m
Offset - source to Channel 800	10140 m
Streamer depth (nominal)	9 m
Sample interval	2 ms
Nominal fold	133
Record length	12 s
Source array depth (nominal)	6 m
Source array volume	5400 cu-in
Shotpoint interval	37.5 m

APB13 Survey	
Vessel	<i>M/V Duke</i>
No. of channels	648
Group length	12.5 m
Offset - source to Channel 1	80 m
Offset - source to Channel 800	8180 m
Streamer depth (nominal)	18 m
Sample interval	2 ms
Nominal fold	108
Record length	10.5 s
Source array depth (nominal)	12 m
Source array volume	3610 cu-in
Shotpoint interval	37.5 m

Processing (key steps, both surveys):

- 2D geometry assignment
- Low pass filter 3 Hz at 18 dB/Octave (two passes)
- Debubble and zero phased designation
- Spherical divergence application (V^2T function)
- Swell noise attenuation, despiking, receiver motion correction, SRME, linear noise attenuation
- Deghosting using ghost wavelet estimation
- Velocity analysis at 1 km interval

- Adjacent trace decimation in shot domain with K filter & NMO wrap
- Radon demultiple
- Diffracted multiple attenuation
- Shot and channel scaling
- First iteration Kirchhoff PSTM
- Migration velocity analysis at 1 km interval
- Pre-migration denoise in common offset domain
- Removal of spherical divergence correction
- Full Kirchhoff PSTM
- High-resolution automatic velocity analysis (50 m interval)
- Radon demultiple
- Denoise in common depth point (CDP) domain
- Angle stack and full stack
- Q compensation and time variant scaling (post stack)
- Source and streamer datum correction (+10 ms for PEG09 survey, +20 ms for APB13 survey)
- Amplitude matching (APB13 scaled by 0.00025 to match PEG09 survey)

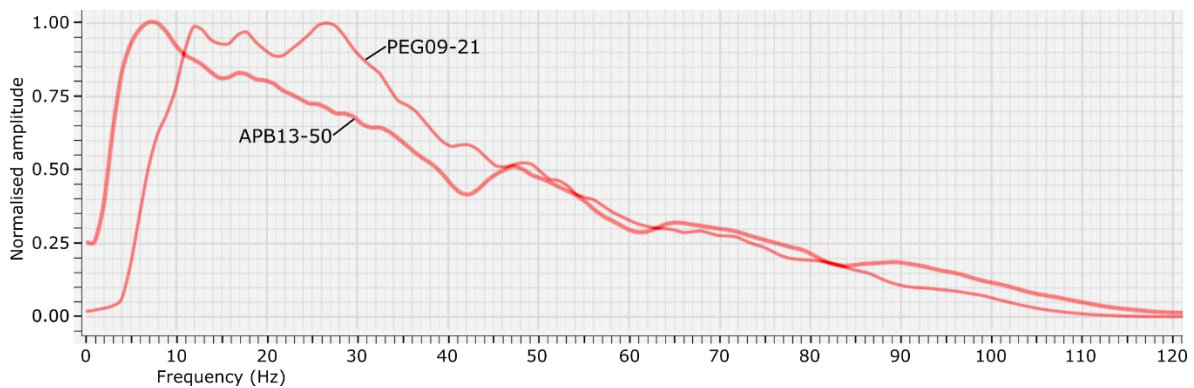


Figure SA-1. Comparison of normalized amplitude spectra from adjacent seismic lines APB13-50 and PEG09-21.

Note: The data we analyzed in this study were the full angle stacks – i.e. where the full range of offsets given in the previous tables are used for imaging. For more information on acquisition and processing of the APB13 and PEG09 surveys, the reader is referred to the complete seismic processing reports listed below.

Acquisition and Processing Reports (PEG09 and APB13 surveys):

- Anardarko New Zealand Ltd (2014). PEP 54858 and PEP 54861 PEG09 PSTM Reprocessing Report 2014. NZP&M, Ministry of Business, Innovation & Employment (MBIE), New Zealand Unpublished Petroleum Report PR4959
- Anardarko New Zealand Ltd (2014). Seismic Data Processing Report - APB-13-2D Pegasus Basin 2D PEP54858. NZP&M, Ministry of Business, Innovation & Employment (MBIE), New Zealand Unpublished Petroleum Report PR5171
- Anardarko New Zealand Ltd (2014). APB-13-2D Pegasus Basin 2D Quality Assurance Report PEP 54861 Marine 2D Seismic Survey PEP 54858. NZP&M, Ministry of Business, Innovation & Employment (MBIE), New Zealand Unpublished Petroleum Report PR5172

Supplement B

Stratigraphic dip at the BGHS

For depth conversion we used a simple 1D velocity function that is consistent with velocity analyses carried out by Crutchley et al. (2015) on Line PEG0923 (one of the lines analyzed in this study). We estimate errors in this velocity function, beneath the seafloor and down to the BGHS, to be less than ± 300 m/s. This velocity function is shown in Figure SB1-A, below. We assume a water velocity of 1500 m/s.

Figure SB1-B-E shows an example of calculating strata-to-BGHS angles from a sub-section of one of the seismic lines.

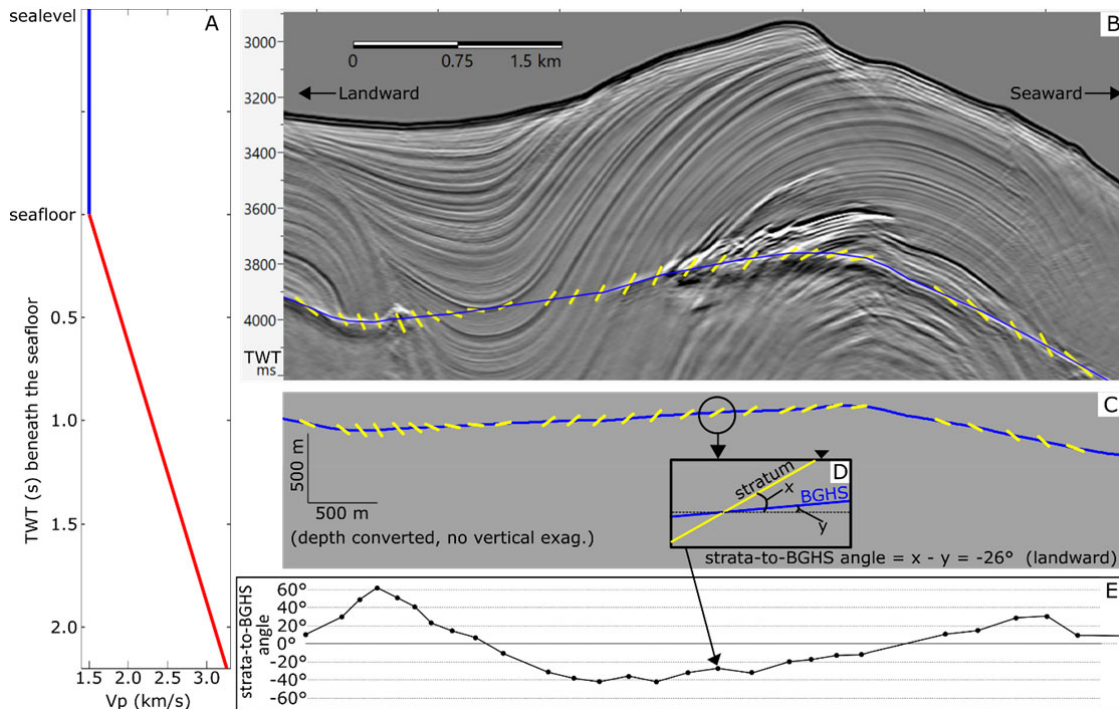


Figure SB1. **A)** The 1D velocity function used to convert time sections to depth. **B)** Section of seismic data where the BGHS is annotated by the blue line and picked stratigraphic reflection segments are in yellow. **C)** 1:1 plot of the BGHS (blue) and the reflection segments (yellow) following depth conversion using the velocity function in (A). **D)** enlargement of a selected stratum-BGHS intersection. In this case, the strata-to-BGHS angle is the absolute dip of the stratum (angle 'x') subtracted by the absolute dip of the BGHS (angle 'y') = -26° (landward dips are negative). **E)** Plot of all strata-to-BGHS angles across this section (black dots). Linear interpolation is used to estimate a continuous profile of strata-to-BGHS angles (black line joining dots).

Errors in strata-to-BGHS angles

The main source of error in estimating strata-to-BGHS angles arises from uncertainties in sub-seafloor velocities and the subsequent depth conversions of the horizon representing the BGHS and the picked strata horizons. By adopting a depth-dependent velocity function beneath the seafloor (Figure SB1-A), we reduce these errors somewhat (in comparison to adopting a constant velocity for sub-seafloor sediments). We estimate peak errors in strata-to-BGHS angles propagating from velocity errors by assuming a conservative error in sub-seafloor velocity of ± 300 m/s (Figure SB2). These angle errors are highest around dips of 45° , reducing significantly at more modest (and more

common) angles. We expect our velocity error to also account for errors in picking seismic reflections.

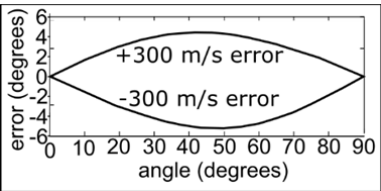


Figure SB2. Estimated error in strata-to-BGHS angles as a function of strata-to-BGHS angle and assuming a velocity error of ± 300 m/s. At 26° (i.e. the angle in Fig. SB1-D), the error is $\sim \pm 4^\circ$.

Another source of error in all angle estimates can come from the fact that seismic sections are not aligned perpendicular to the strike of geological structures (i.e. apparent dip versus real dip). To assess these errors, we mapped out hinge lines of anticlines and synclines in the closely spaced 2D data to have an approximation of the range of strikes of the folded strata in the study area (Figure SB3). The “worst” orientation of lines with respect to underlying structure is $\sim 10^\circ$ (Figure SB3, Inset A), which amounts to a peak error in apparent dip of less than 0.5° (Figure SB3, Inset B).

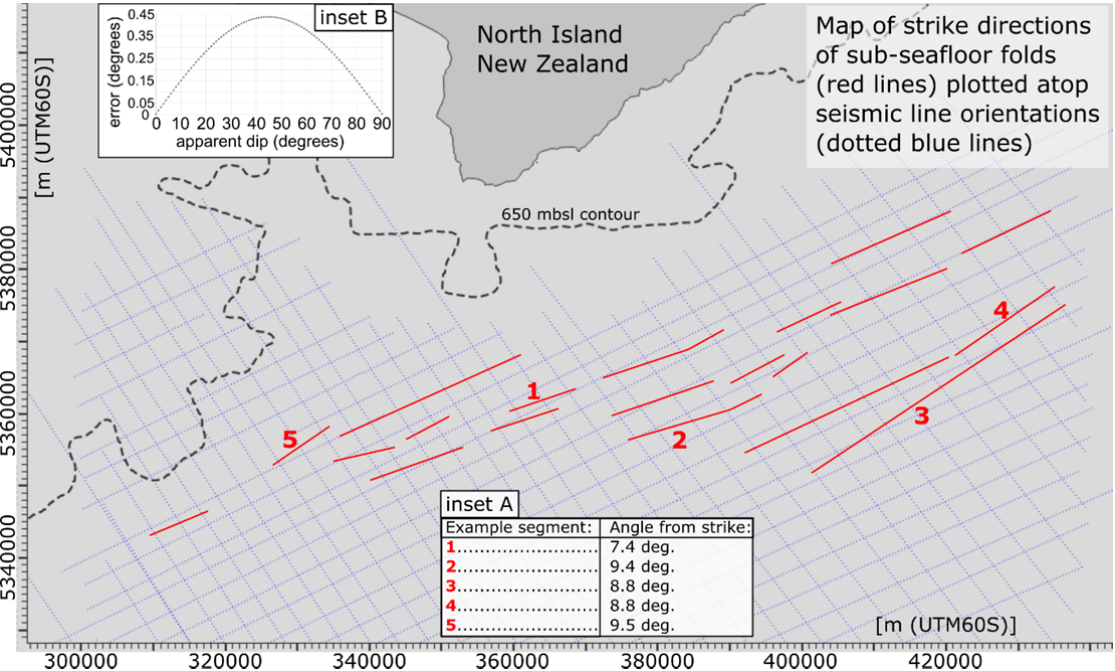
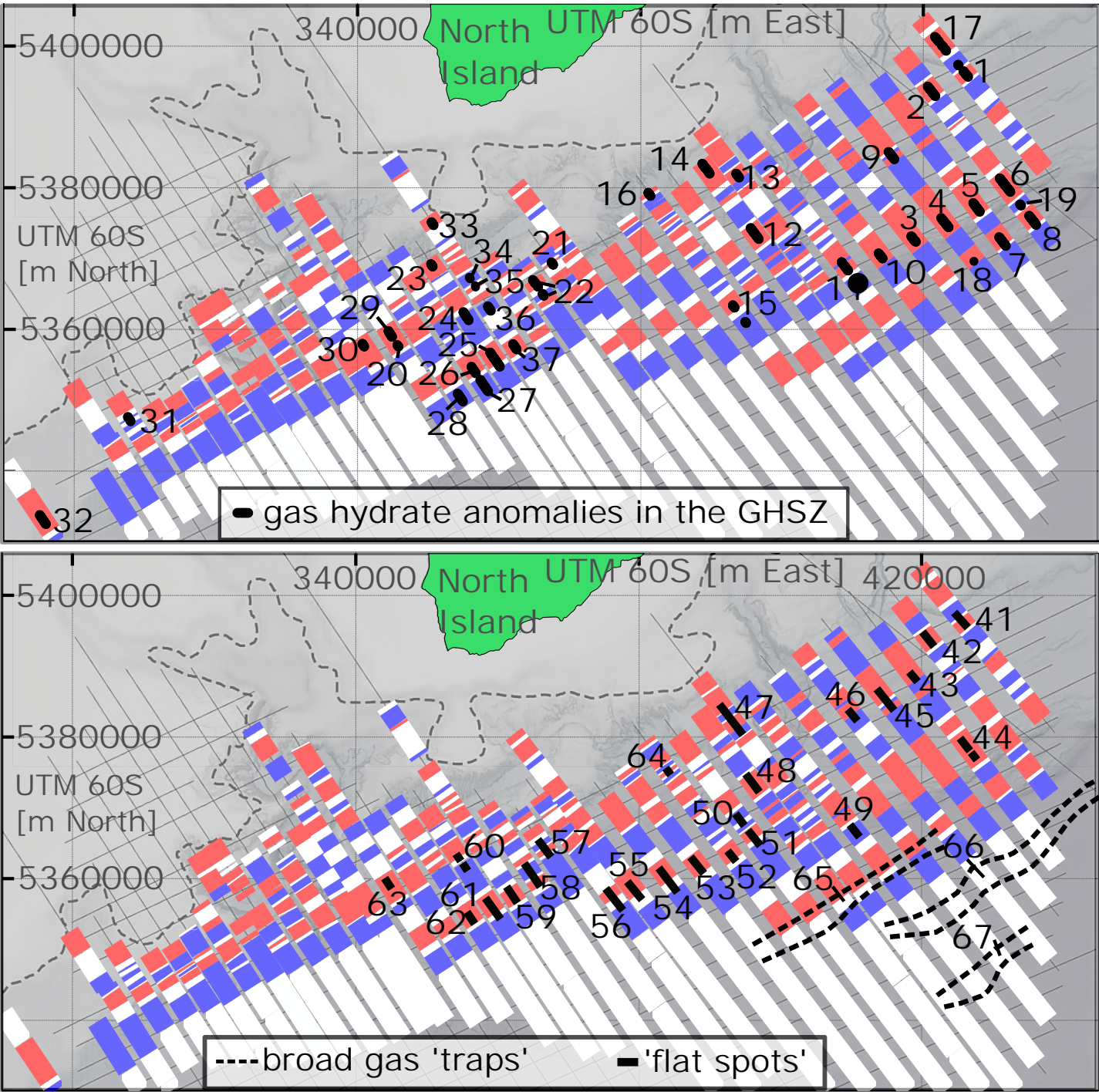


Figure SB3. Strike analysis of anticline and syncline hinges (red lines). Selected strike lines at higher angles to the seismic network are numbered. **Inset A)** The inset table shows the angle between the \sim NW-SE trending seismic network and the dip direction (i.e. direction normal to strike) at each strike line. **Inset B)** Error from non-ideal alignment of seismic lines with respect to true dip direction of geological structures. This graph is calculated for a mis-orientation of 10° (i.e. the greatest angle in the table in Inset A).

Gas and gas hydrate features



These are the maps of gas and gas hydrate observations from Figure 2 of the manuscript. The features are numbered. Seismic section extracts from each of these numbered features are shown in the following pages of this supplement.

Note for the following pages of this supplement:

On pages 2 and 3 of this supplement: cyan arrows point to anomalous negative-polarity reflectivity above the BGHS, implying the existence of free gas within the gas hydrate stability zone (GHSZ). Yellow arrows mark leading positive polarity indicative of concentrated gas hydrates (and presumably no, or very little, free gas).
On pages 4 and 5 of this supplement: yellow arrows point to flat spots beneath the BGHS. Dotted polygons on page 5 outline broad gas accumulations in gently-dipping strata.

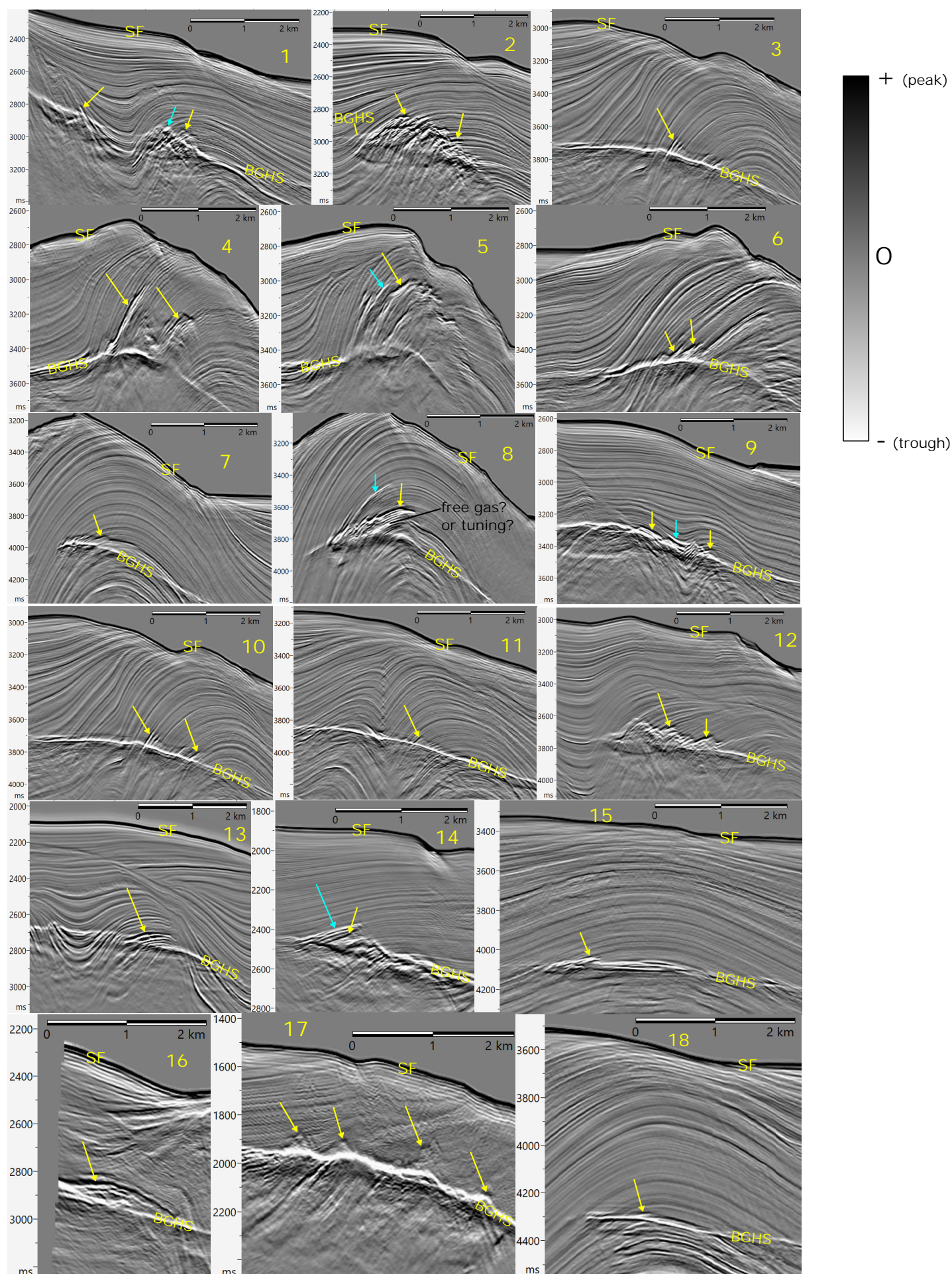
Closely bedded layers lead to tuning effects that can make it difficult to distinguish the relative importance of free gas and gas hydrate in contributing to anomalous reflectivity. Number 8 (following page) is a good example, where there is a negative polarity reflection between the BGHS and an overlying positive polarity reflection. The negative polarity reflection could be attributable to free gas, but alternatively, wavelet interference (tuning) could be the main reason for this seismic manifestation. This could happen as the wavelet passes through relatively fine-scale bedding of more-concentrated / less-concentrated gas hydrates in, e.g., sands and shales.

Supplementary Material C (Page 2 of 5)

Arrows point to examples of anomalous reflectivity above the BSR. Cyan arrows mark negative polarity reflections and imply the existence of free gas within the gas hydrate stability zone (GHSZ). Yellow arrows mark leading positive polarity indicative of concentrated gas hydrates (and presumably no, or very little, free gas).

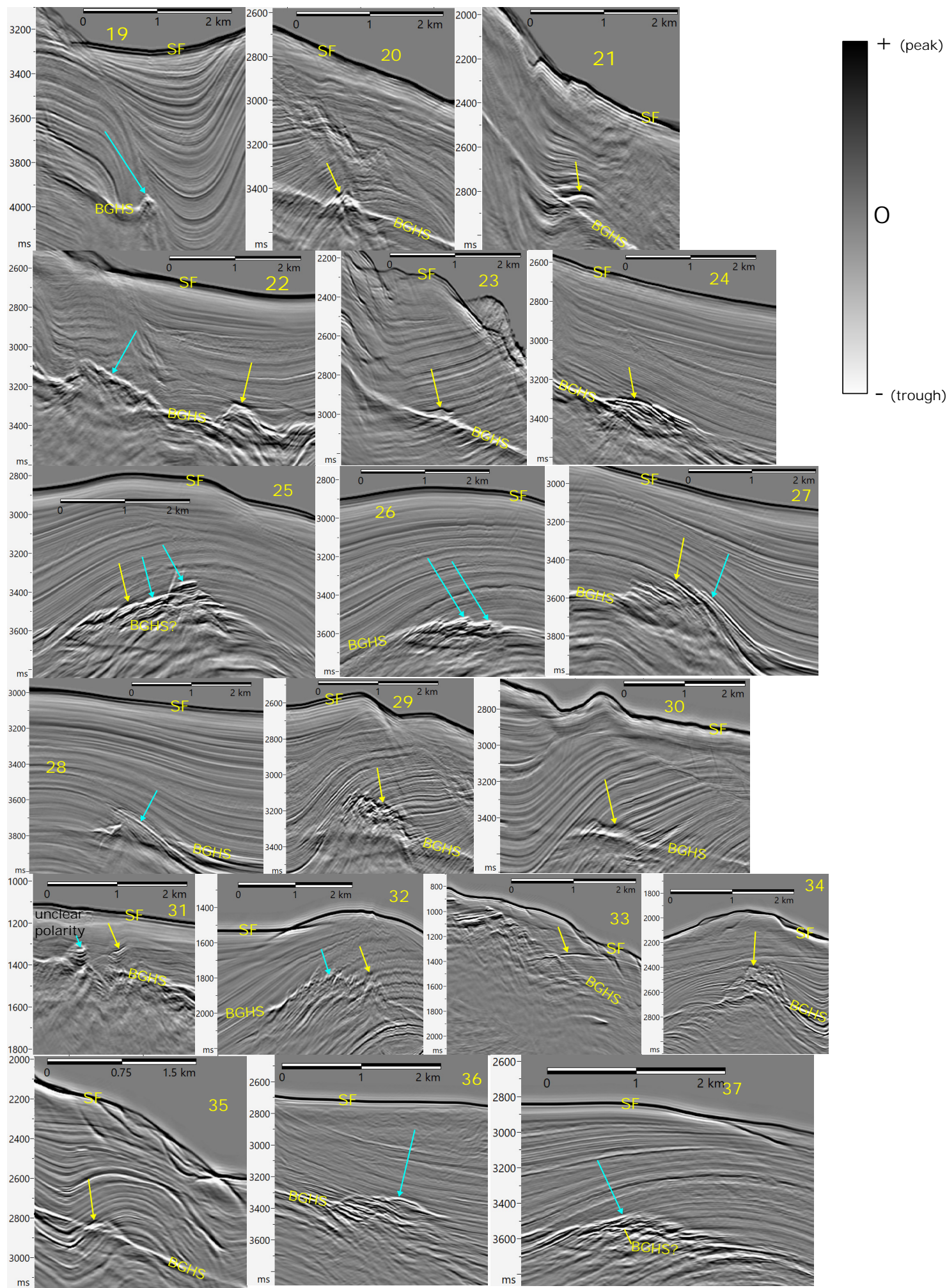
Note: Polarity follows SEG normal convention (i.e. increase in impedance = peak; decrease in impedance = trough)

SF = seafloor, BGHS = base of gas hydrate stability



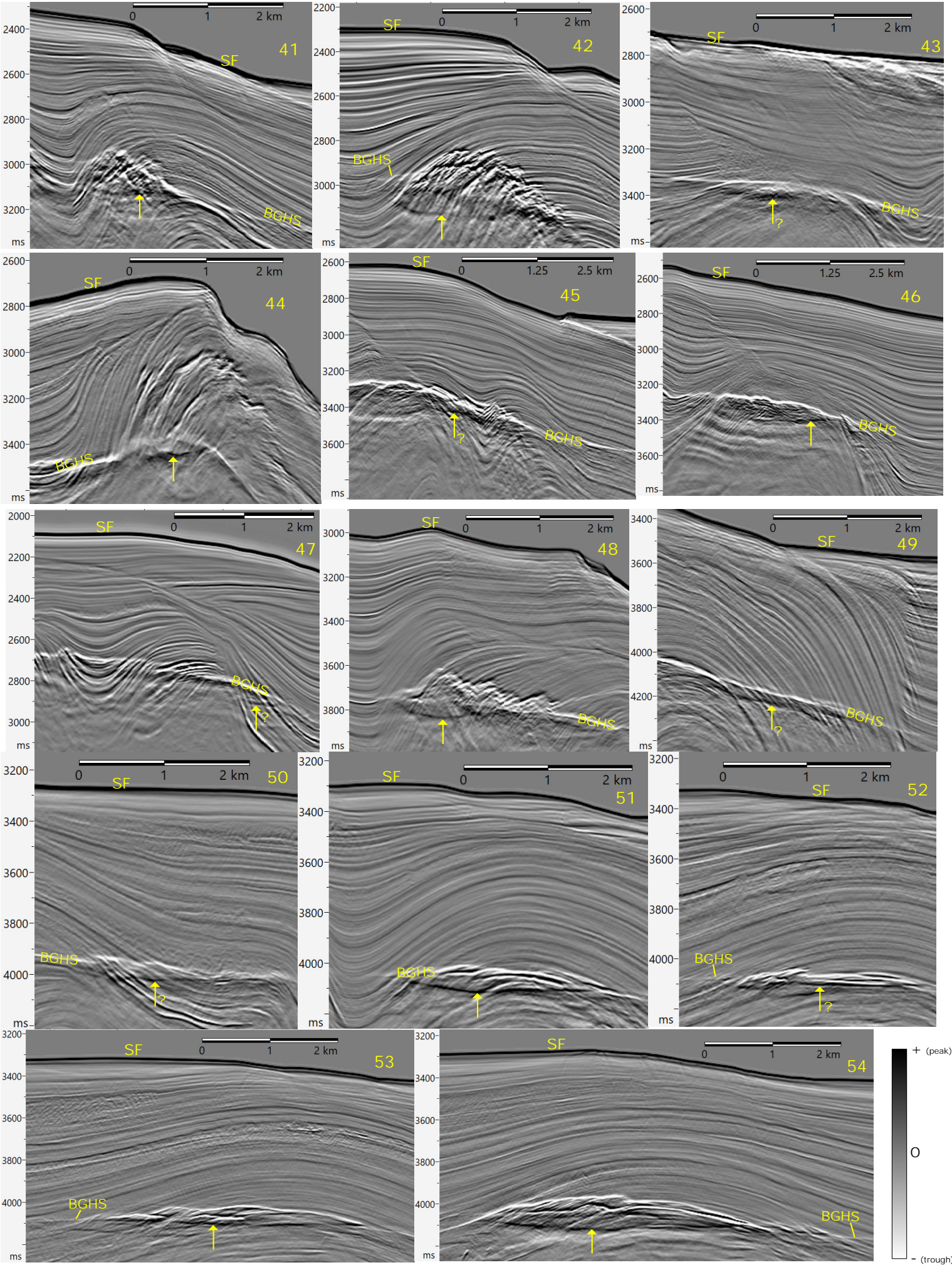
Supplemenatry Material C (Page 3 of 5)

Arrows point to examples of anomalous reflectivity above the BSR. Cyan arrows mark negative polarity reflections and imply the existence of free gas within the gas hydrate stability zone (GHSZ). Yellow arrows mark leading positive polarity indicative of concentrated gas hydrates (and presumably no, or very little, free gas).



Supplemenatry Material C (Page 4 of 5)

(Yellow arrows point to flat spots; question marks denote more tenuous interpretations)



Supplemenatry Material C (Page 5 of 5)

(Yellow arrows point to flat spots; question marks denote more tenuous interpretations)
(dotted polygons outline broad gas accumulations in gently-dipping strata)

